Journal of Photochemistry and Photobiology A: Chemistry 230 (2012) 15–22

Contents lists available at SciVerse ScienceDirect

Journal of Photochemistry and Photobiology A: Chemistry

journal homepage: www.elsevier.com/locate/jphotochem

Preparation of Cu-doped $Cd_{0.1}Zn_{0.9}S$ solid solution by hydrothermal method and its enhanced activity for hydrogen production under visible light irradiation

Melody Kimi[a], Leny Yuliati[b,*], Mustaffa Shamsuddin[a]

[a] Department of Chemistry, Faculty of Science, Universiti Teknologi Malaysia, 81310 UTM Skudai, Johor, Malaysia
[b] Ibnu Sina Institute for Fundamental Science Studies, Universiti Teknologi Malaysia, 81310 UTM Skudai, Johor, Malaysia

ARTICLE INFO

Article history:
Received 30 September 2011
Received in revised form
12 December 2011
Accepted 7 January 2012
Available online 14 January 2012

Keywords:
Cu-doped $Cd_{0.1}Zn_{0.9}S$
Hydrothermal
Co-precipitation
Visible light
Hydrogen production

ABSTRACT

A series of Cu-doped $Cd_{0.1}Zn_{0.9}S$ solid solution with various amounts of Cu dopant was successfully prepared by hydrothermal method. The properties and the photocatalytic activity of the prepared samples for hydrogen production under visible light irradiation were compared to those prepared by co-precipitation method. The Cu-doped $Cd_{0.1}Zn_{0.9}S$ samples prepared by hydrothermal method showed both improved crystallinity and photoabsorption ability as compared to the undoped sample. On the other hand, even though Cu-doped $Cd_{0.1}Zn_{0.9}S$ prepared by co-precipitation method also showed improved photoabsorption ability in the visible light region, the samples showed poor crystallinity compared to the undoped one. With the same amount of Cu dopant, all samples prepared by hydrothermal method were found to exhibit higher photocatalytic activity for hydrogen production than the samples prepared by co-precipitation method. It was revealed that the amount of Cu dopant, crystallinity and narrow band gap energy are important factors to obtain highly active and stable photocatalysts.

1. Introduction

Semiconductor photochemistry is one research field that plays important role in various photocatalytic applications. As example, photocatalytic hydrogen production from water on a semiconductor has been a great interesting challenge for researchers to convert solar energy into clean and renewable hydrogen energy. In order to utilize solar energy efficiently, development of visible light active semiconductor is crucial. For such reason, photochemistry of the semiconductor such as band structure must be controlled. Proper conduction band position is important to provide high potential energy for reduction of water to hydrogen. Two possible methods which are most commonly used to control band structure are doping with foreign elements and forming solid solution between wide and narrow band gap semiconductors [1–9].

One of the most extensively studied sulfides solid solutions is $Cd_xZn_{1-x}S$ due to its controllable band structure and excellent performance under visible light irradiation [1–5]. Although $Cd_xZn_{1-x}S$ was successful to overcome shortcomings of photocorrosion from CdS and wide band gap energy of ZnS, the band gap energy of this solid solution was still large, thus limited the utilization of photon energy for hydrogen evolution under visible light irradiation. Recently, doping of $Cd_xZn_{1-x}S$ solid solution with various metal ions have been reported, such as Cu [10–13] and Ni [14,15] to further improve the efficiency of $Cd_xZn_{1-x}S$. It was reported that Cu^{2+} and Ni^{2+} can contribute to the enhancement in the visible light response of the $Cd_xZn_{1-x}S$ photocatalyst by reducing the band gap energy [10–15].

In addition to the band gap engineering, the method to prepare a photocatalyst itself is very significant since it can affect the properties, thus affect the photocatalytic activity. Some studies revealed that different preparation methods lead to different photocatalytic activity due to the differences in the physical chemical properties [16,17]. Even though prepared by the same co-precipitation method, $Cd_{1-x}Zn_xS$ annealed at different temperatures showed different photocatalytic activities for hydrogen evolution [16]. Recently, we found that $Cd_{0.1}Sn_xZn_{0.9-x}S$ photocatalysts prepared by hydrothermal method showed higher photocatalytic activity and stability compared to the ones prepared by co-precipitation method [17].

On the other hand, some research groups have reported the preparation of Cu-doped $Cd_{0.1}Zn_{0.9}S$ series by co-precipitation method [10–13]. However, other method to prepare Cu-doped $Cd_{0.1}Zn_{0.9}S$ series has never been reported yet. Therefore, there are lack of alternative preparation methods as well as comparison studies on properties and photocatalytic performance of the photocatalysts prepared by different methods. In the present paper, we demonstrate that Cu-doped $Cd_{0.1}Zn_{0.9}S$ can be prepared by hydrothermal method for the first time, and the prepared samples have much higher activity than those prepared by co-precipitation method for hydrogen production under visible light irradiation. Based on the comparison study between properties

* Corresponding author. Tel.: +60 7 5536272; fax: +60 7 5536080.
E-mail address: leny@ibnusina.utm.my (L. Yuliati).

1010-6030/$ – see front matter © 2012 Elsevier B.V. All rights reserved.
doi:10.1016/j.jphotochem.2012.01.004

and photocatalytic activity of Cu-doped $Cd_{0.1}Zn_{0.9}S$ series prepared by hydrothermal and co-precipitation methods, important factors contributing to the high photocatalytic activity and stability of Cu-doped $Cd_{0.1}Zn_{0.9}S$ series are revealed.

2. Experimental

2.1. Synthesis of photocatalysts

Cu-doped $Cd_{0.1}Zn_{0.9}S$ samples were prepared by two methods, *i.e.*, hydrothermal and co-precipitation methods. The samples were labeled to as Cu(x)-doped $Cd_{0.1}Zn_{0.9}S$, with x showed the doping amount of Cu. For hydrothermal method, a series of Cu-doped $Cd_{0.1}Zn_{0.9}S$ samples was prepared in a similar way to the previous literatures [14,17]. In a typical synthesis for Cu(0.01)-doped $Cd_{0.1}Zn_{0.9}S$, 0.2 mmol of $Cu(NO_3)_2{\cdot}3H_2O$ (Fluka, 98%), 2 mmol of $Cd(NO_3)_2{\cdot}4H_2O$ (Aldrich, 98%), 18 mmol of $Zn(CH_3COO)_2{\cdot}2H_2O$ (GCE chemicals, 98%) and 20 mmol of CH_3CSNH_2 (Merck, 99%) were dissolved in 50 mL of distilled water. The solution was added into an autoclave that was sealed and heated in an oven at 433 K for 8 h. After natural cooling to room temperature, the precipitates were washed with distilled water for several times and dried in vacuum at room temperature.

For co-precipitation method, the series of Cu-doped $Cd_{0.1}Zn_{0.9}S$ was prepared similarly to the previous studies [11–13,17]. Typically, to synthesize Cu(0.01)-doped $Cd_{0.1}Zn_{0.9}S$, 50 mL of 2 mol $Na_2S{\cdot}xH_2O$ (Q Rëc, 98%) was added drop wise to a mixture containing 0.01 mol of $Cu(NO_3)_2{\cdot}3H_2O$ (Fluka, 98%), 0.1 mol of $Cd(NO_3)_2{\cdot}4H_2O$ (Aldrich, 98%) and 0.9 mol of $Zn(CH_3COO)_2{\cdot}2H_2O$ (GCE chemicals, 98%) dissolved in 50 mL distilled water. The mixed solution was stirred for 12 h at room temperature. The resulting precipitate was filtered and washed several times by distilled water. The product then was dried in air at 343 K for 12 h.

2.2. Characterizations of photocatalysts

The diffraction patterns of the prepared samples were investigated by X-ray powder diffraction (XRD) using Bruker Advance D8 Siemens 5000 diffractometer, with Cu Kα radiation (λ = 0.15418 nm, 40 kV, 40 mA). The diffuse reflectance UV–visible (DR UV–vis) spectra were recorded on a Perkin Elmer Ultraviolet-visible Spectrometer Lambda 900. Barium sulfate ($BaSO_4$) was used as the reference. The morphologies and nanocrystal sizes of the samples were observed with field emission scanning electron microscopy (FESEM) using JEOL JSM 6701F with platinum coating (2 kV, 10 mA).

2.3. Photocatalytic activity evaluation

Photocatalytic hydrogen evolution was performed in a closed-side irradiated-Pyrex cell equipped with a water condenser to maintain the temperature constant during the reaction [17]. A 500 W halogen lamp was used as the visible light source. Hydrogen gas evolved was identified by an online system with thermal conductivity detector (TCD) gas chromatography (GC, Agilent 7890A) using Supelco 13X molecular sieves and argon carrier gas, which amount was measured by volumetric method. In all experiments, the powder sample (0.2 g) was dispersed by magnetic stirring in an aqueous solution (50 mL) containing 0.25 M Na_2SO_3 and 0.35 M Na_2S [18] as sacrificial agents. Nitrogen gas was purged through the reaction cell for 30 min before reaction to remove air. In order to check the photocatalytic stability, the sample was reused without washing or drying. Before another 5 h-irradiation in the second run, the reactor containing the tested sample was purged with nitrogen gas for 30 min to ensure that there was no hydrogen product remained in the reactor.

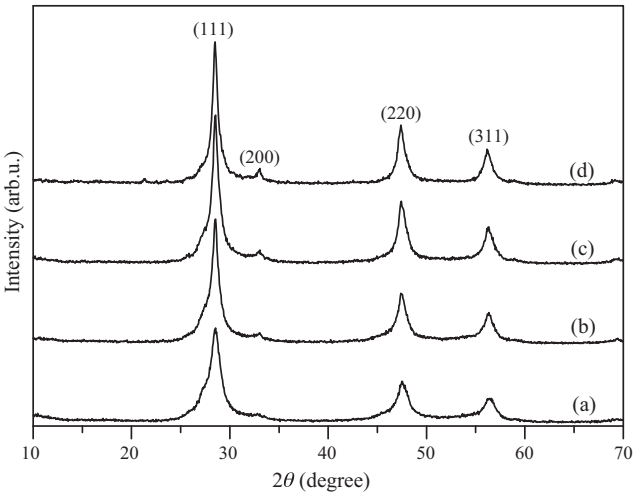

Fig. 1. XRD patterns of (a) $Cd_{0.1}Zn_{0.9}S$, (b) Cu(0.01)-doped $Cd_{0.1}Zn_{0.9}S$, (c) Cu(0.03)-doped $Cd_{0.1}Zn_{0.9}S$, and (d) Cu(0.05)-doped $Cd_{0.1}Zn_{0.9}S$ prepared by hydrothermal method.

3. Results and discussion

3.1. Crystal structure and morphology

The XRD patterns of $Cd_{0.1}Zn_{0.9}S$ and Cu-doped $Cd_{0.1}Zn_{0.9}S$ prepared by hydrothermal method are depicted in Fig. 1. All samples exhibit major diffraction peaks at 2θ of 28.6, 32.5, 47.6 and 56.3, corresponding to the (1 1 1), (2 0 0), (2 2 0) and (3 1 1) planes respectively, which is a typical pattern of cubic zinc blende phase [10–15,19,20]. There was a very small peak observed at 2θ = 27 which corresponded to CdS (JCPDS 241126). It can be suggested that a mixture of cubic $Cd_{0.1}Zn_{0.9}S$ solid solution and CdS may exist in the samples. The diffraction peaks of all samples prepared by hydrothermal method are intense, suggesting that the obtained products, Cu-doped $Cd_{0.1}Zn_{0.9}S$, are well crystallized under the present synthesis condition. As the amount of Cu dopant increased from 0.01 to 0.05 mol, the peak intensity increased. This result indicates that there is an increase in the crystallinity of the samples,

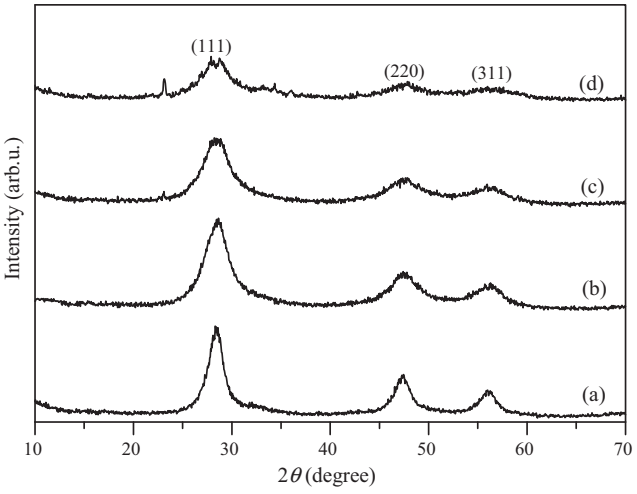

Fig. 2. XRD patterns of (a) $Cd_{0.1}Zn_{0.9}S$, (b) Cu(0.01)-doped $Cd_{0.1}Zn_{0.9}S$, (c) Cu(0.03)-doped $Cd_{0.1}Zn_{0.9}S$, and (d) Cu(0.05)-doped $Cd_{0.1}Zn_{0.9}S$ prepared by co-precipitation method.

Table 1
Properties of $Cd_{0.1}Zn_{0.9}S$ and Cu-doped $Cd_{0.1}Zn_{0.9}S$ samples.

Entry	Samples	d_{111} value[c] (Å)	Lattice constant, a[d] (Å)	Crystallite size, d[e] (nm)	Band gap (eV)[f]
1[a]	$Cd_{0.1}Zn_{0.9}S$	3.1281	5.4181	6.87	3.11
2[a]	Cu(0.01)-doped $Cd_{0.1}Zn_{0.9}S$	3.1281	5.4181	10.35	2.85
3[a]	Cu(0.03)-doped $Cd_{0.1}Zn_{0.9}S$	3.1281	5.4181	11.29	2.84
4[a]	Cu(0.05)-doped $Cd_{0.1}Zn_{0.9}S$	3.1281	5.4181	13.05	2.78
5[b]	$Cd_{0.1}Zn_{0.9}S$	3.1167	5.3982	5.04	2.94
6[b]	Cu(0.01)-doped $Cd_{0.1}Zn_{0.9}S$	–	–	3.23	2.79
7[b]	Cu(0.03)-doped $Cd_{0.1}Zn_{0.9}S$	–	–	3.17	2.75
8[b]	Cu(0.05)-doped $Cd_{0.1}Zn_{0.9}S$	–	–	2.93	2.63

[a] Samples were prepared by hydrothermal method.
[b] Samples were prepared by co-precipitation method.
[c] The value was calculated from $2d_{111}\sin\theta = n\lambda$, not applicable for Entries 6–8, see the text.
[d] The value was calculated from $a = d_{111}\sqrt{3}$, not applicable for Entries 6–8, see the text.
[e] The value was calculated from Scherrer equation.
[f] The value was obtained from Tauc Plot.

suggesting that the addition of Cu might promote the growth of the crystals. The increase in the crystallinity was also observed for Cu [21] and other metal [22] doped compounds due to the metal-induced crystallization effect. There is no peak shifting when Cu was doped into $Cd_{0.1}Zn_{0.9}S$, indicating that Cu was successfully doped into the $Cd_{0.1}Zn_{0.9}S$ lattice without causing crystal distortion since Cu^{2+} (0.72 Å) and Zn^{2+} (0.74 Å) have similar ionic radii. The substitution of Zn^{2+} by Cu^{2+} is also favorable in terms of charge balance.

The crystal properties of the samples prepared by hydrothermal method are shown in Table 1 (Entries 1–4). The lattice constants (a) of the samples were calculated by determining d-spacing of (1 1 1) peak using Bragg's law (see Table 1, captions c and d for the details). The lattice constant of $Cd_{0.1}Zn_{0.9}S$ was higher than that of cubic ZnS prepared with the same method (a = 5.3852), suggesting the successful insertion of Cd ions into the ZnS lattice to form the $Cd_{0.1}Zn_{0.9}S$ solid solution. On the other hand, the values of lattice parameter and d-spacing of $Cd_{0.1}Zn_{0.9}S$ were not changed when Cu was doped into $Cd_{0.1}Zn_{0.9}S$. The crystallite size were estimated using the most intense (1 1 1) peak by Scherrer equation. As the amount of Cu dopant increased, the crystallite size increased. These results confirmed that Cu dopant promoted the growth of

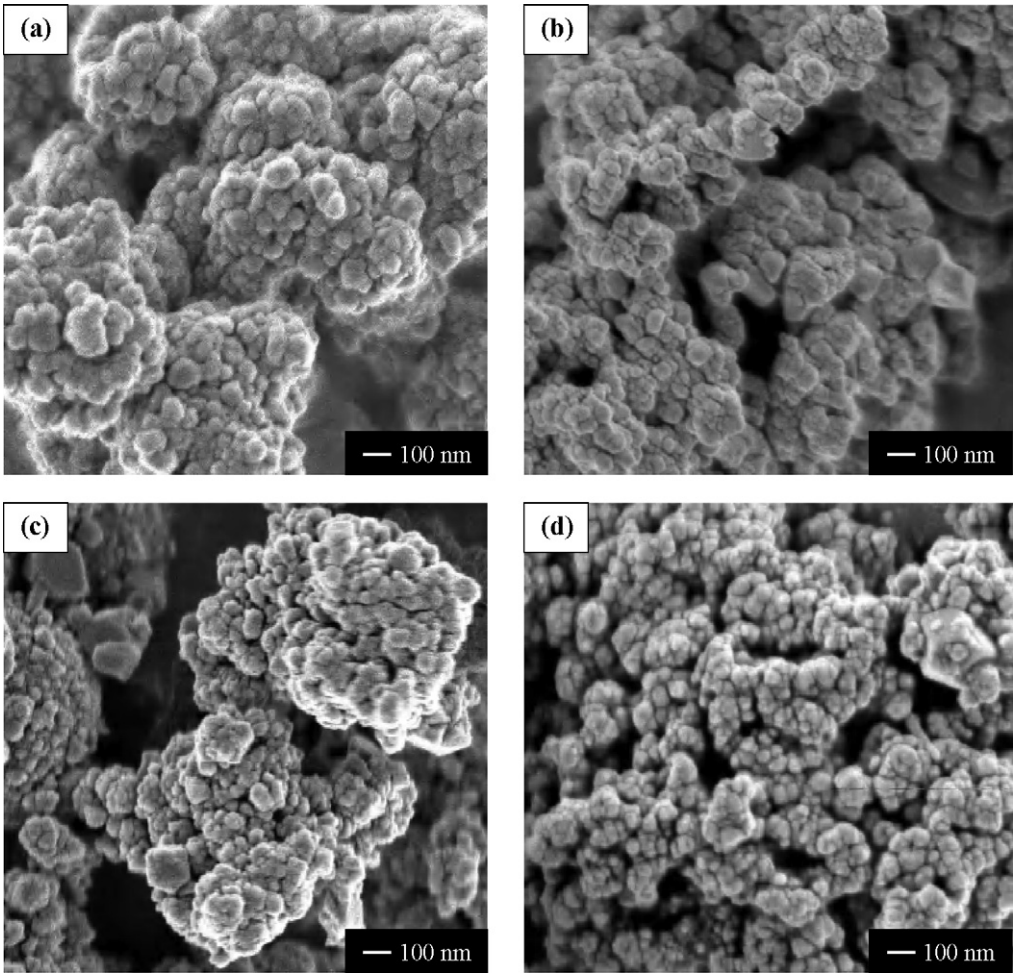

Fig. 3. FESEM images of (a) $Cd_{0.1}Zn_{0.9}S$, (b) Cu(0.01)-doped $Cd_{0.1}Zn_{0.9}S$, (c) Cu(0.03)-doped $Cd_{0.1}Zn_{0.9}S$, and (d) Cu(0.05)-doped $Cd_{0.1}Zn_{0.9}S$ prepared by hydrothermal method.

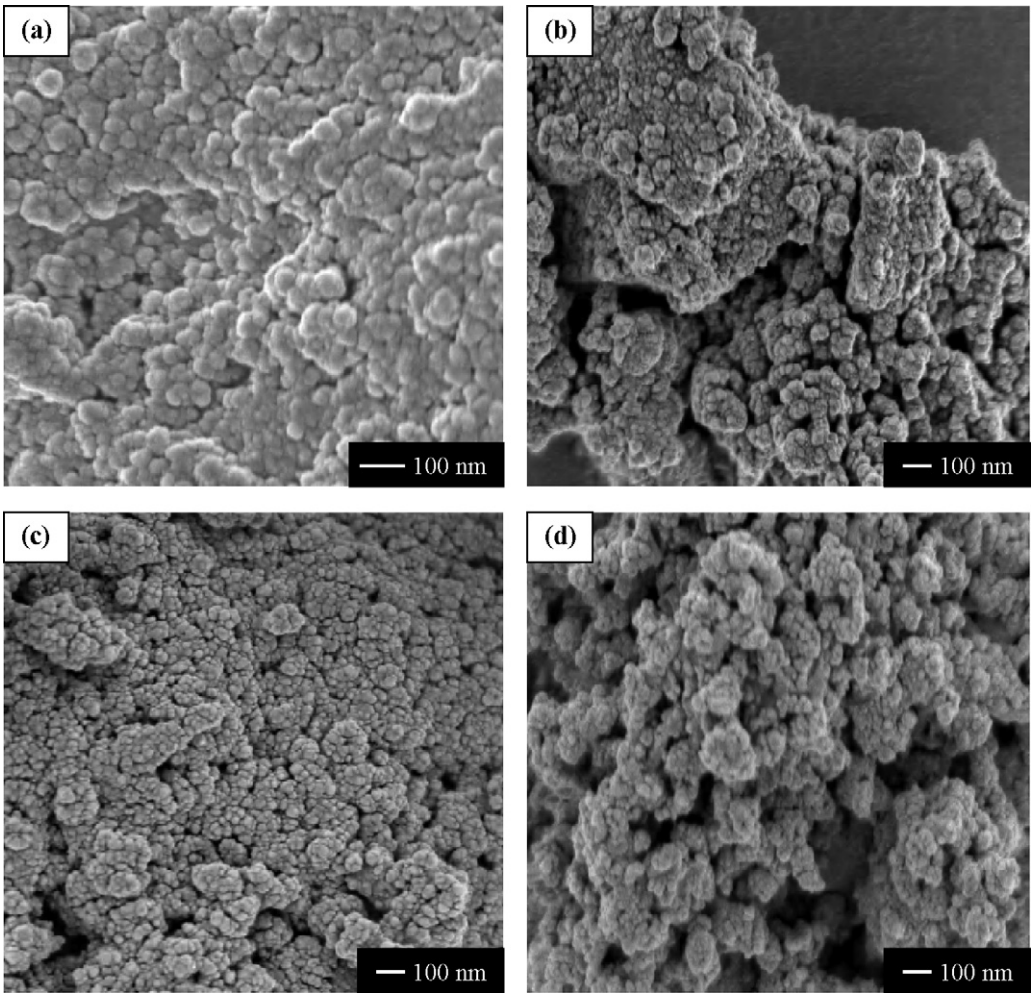

Fig. 4. FESEM images of (a) $Cd_{0.1}Zn_{0.9}S$, (b) Cu(0.01)-doped $Cd_{0.1}Zn_{0.9}S$, (c) Cu(0.03)-doped $Cd_{0.1}Zn_{0.9}S$, and (d) Cu(0.05)-doped $Cd_{0.1}Zn_{0.9}S$ prepared by co-precipitation method.

$Cd_{0.1}Zn_{0.9}S$ crystal when the samples were prepared by hydrothermal method.

Fig. 2 shows the XRD patterns of $Cd_{0.1}Zn_{0.9}S$ and Cu-doped $Cd_{0.1}Zn_{0.9}S$ prepared by co-precipitation method. The XRD patterns were similar to those of the samples prepared by hydrothermal method. For $Cd_{0.1}Zn_{0.9}S$ and Cu(0.01)-doped $Cd_{0.1}Zn_{0.9}S$ samples, there are three major diffraction peaks at 2θ of 28.6, 47.6 and 56.3, corresponding to the (1 1 1), (2 2 0) and (3 1 1) planes of cubic zinc blende phase. However, when the amount of Cu dopant increased, the diffraction peak of (1 1 1) plane was broadened and additional peaks at 2θ of 23–33 were observed, that would be due to the presence of hexagonal phase. It is well known that $Cd_xZn_{1-x}S$ can exist in both hexagonal and cubic phases [19,20,23]. It was revealed that hexagonal phase was observed when the amount of Zn in $Cd_xZn_{1-x}S$ was small [19,23]. In the present study, we also obtained that the hexagonal phase was formed when the amount of Zn decreased due to the increase of Cu dopant amount. This result is different from the case of hydrothermal method; it seems that addition of Cu dopant by co-precipitation method affected the formation of crystal phase in the samples.

Fig. 2 also shows that as the amount of Cu dopant increased, the peak at (1 1 1) seemed to be shifted to higher 2θ. This was due to the formation of hexagonal phase as mentioned above. Since the cubic (1 1 1) and the hexagonal (0 0 2) lines coincide, it is very difficult to differentiate the cubic from the hexagonal structure [20]. However, it is clear that the XRD peaks were broadened as the amount of Cu dopant increased. Based on the calculation by Scherrer equation, crystallite size decreased as the amount of Cu dopant increased (Table 1, Entries 5–8). Different from hydrothermal method, the effect of metal induced crystallization was not observed when using co-precipitation method, which might be due to low temperature used in the synthesis.

Fig. 3 shows FESEM images of $Cd_{0.1}Zn_{0.9}S$ and Cu-doped $Cd_{0.1}Zn_{0.9}S$ prepared by hydrothermal method. It can be observed that all these samples consisted of nanospheres in the range of 20–120 nm, which agglomerated with no uniform size. The surface composition of the samples were analyzed by EDS and it was confirmed that Cu was present in all samples. However, the addition of Cu did not change the morphology of $Cd_{0.1}Zn_{0.9}S$. FESEM images of samples prepared by co-precipitation method are shown in Fig. 4. Similar to the samples prepared by hydrothermal method, there was no obvious change in morphology structure when Cu was added into $Cd_{0.1}Zn_{0.9}S$. The samples showed non uniform sphere shape with the size of *ca.* 10–50 nm which was slightly smaller than the average size of the samples prepared by hydrothermal method. This result agrees well with the results from XRD patterns.

3.2. Optical properties

Fig. 5 displays DR UV–vis absorption spectra of the samples prepared by hydrothermal method. All of these samples possess absorption edges in the visible light region. The $Cd_{0.1}Zn_{0.9}S$ sample showed a visible light absorption band with a shoulder peak around 400–500 nm. The similar feature of unsmooth absorption

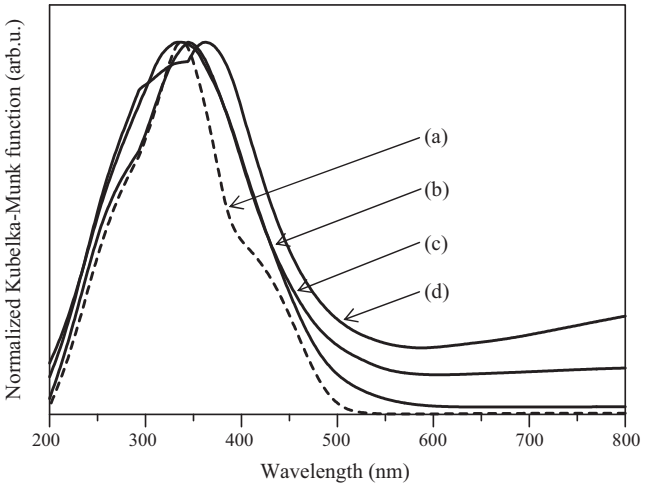

Fig. 5. DR UV–vis spectra of (a) $Cd_{0.1}Zn_{0.9}S$, (b) Cu(0.01)-doped $Cd_{0.1}Zn_{0.9}S$, (c) Cu(0.03)-doped $Cd_{0.1}Zn_{0.9}S$, and (d) Cu(0.05)-doped $Cd_{0.1}Zn_{0.9}S$ prepared by hydrothermal method.

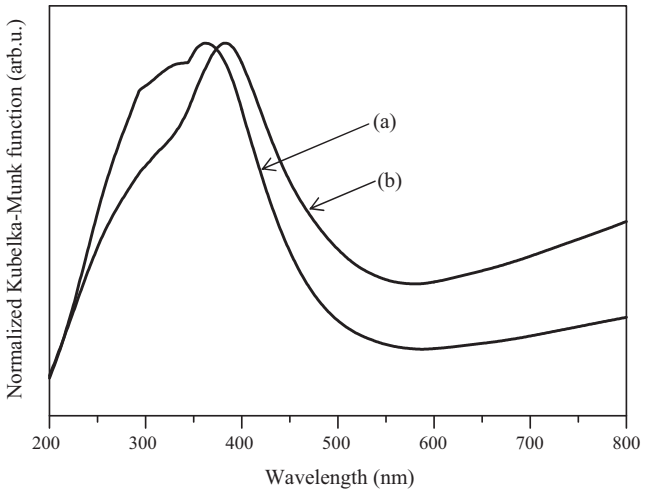

Fig. 7. DR UV–vis spectra of (a) Cu(0.05)-doped $Cd_{0.1}Zn_{0.9}S$ prepared by hydrothermal method and (b) Cu(0.05)-doped $Cd_{0.1}Zn_{0.9}S$ prepared by co-precipitation method.

spectrum for $Cd_{0.1}Zn_{0.9}S$ sample has also been observed in the literatures [10,18,24]. In good agreement with XRD pattern, this result again suggested that the formation of solid solution between CdS and ZnS was not very straight forward, as also previously mentioned in the literature [10]. The addition of Cu dopant extended the visible light absorption of $Cd_{0.1}Zn_{0.9}S$ to longer wavelength. As shown in Fig. 5, with increasing amount of Cu dopant, red shift of absorption edge was continuously observed; the absorption edge of Cu(0.01)-doped $Cd_{0.1}Zn_{0.9}S$ was around 550 nm, followed by Cu(0.03)-doped $Cd_{0.1}Zn_{0.9}S$ at around 600 nm and Cu(0.05)-doped $Cd_{0.1}Zn_{0.9}S$ at around 650 nm. However, large absorption tail around 600–800 nm was also clearly observed on Cu(0.03)-doped $Cd_{0.1}Zn_{0.9}S$ and Cu(0.05)-doped $Cd_{0.1}Zn_{0.9}S$ samples, which increased along with the increase of Cu dopant amount. It was proposed that the absorption at 600–800 nm could be assigned to the Cu^{2+} *d–d* transition [25]. Similar results have been reported for other Cu-doped CdS–ZnS solid solution [10–13] and in the case of Cu-doped ZnS samples [6,26].

The diffuse reflectance spectra of samples prepared by co-precipitation method are shown in Fig. 6. The absorption edge of $Cd_{0.1}Zn_{0.9}S$ was about 470 nm; this value was similar to the one reported by other group [13]. When the amount of added Cu increased, the absorption edge shifted to longer wavelength in visible light region. Similar to the samples prepared by hydrothermal method, Cu(0.03)-doped $Cd_{0.1}Zn_{0.9}S$ and Cu(0.05)-doped $Cd_{0.1}Zn_{0.9}S$ showed a large absorption tail at 600–800 nm which might be due to the presence of Cu^{2+} *d–d* transition [25].

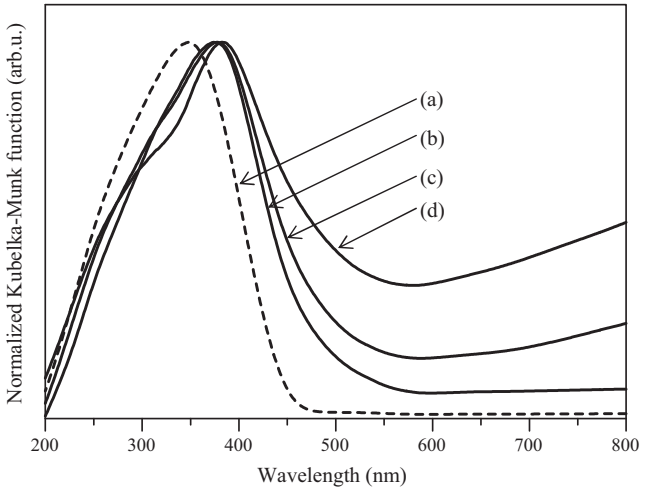

Fig. 6. DR UV–vis spectra of (a) $Cd_{0.1}Zn_{0.9}S$, (b) Cu(0.01)-doped $Cd_{0.1}Zn_{0.9}S$, (c) Cu(0.03)-doped $Cd_{0.1}Zn_{0.9}S$, and (d) Cu(0.05)-doped $Cd_{0.1}Zn_{0.9}S$ prepared by co-precipitation method.

For Cu doping, different preparation method has been reported to give different absorption spectrum in the region of Cu^{2+} *d–d* transition [27]. As also found in our case, the difference was more obvious when the amount of Cu doping was high. Even though the same amount of Cu dopant was introduced, a higher absorption at 600–800 nm was observed on samples prepared by co-precipitation method. For comparison, representatively the absorption spectra of Cu(0.05)-doped $Cd_{0.1}Zn_{0.9}S$ samples prepared by hydrothermal and co-precipitation method is shown in Fig. 7. It has been reported that during Cu doping process, Cu might exist as Cu^{2+} and Cu^{+} [28–30]. In addition to *d–d* transition, Cu^{2+} also has absorption at 440 nm, while Cu^{+} does not have *d–d* transition, but has absorption range from UV up to 320 nm [31]. It can be suggested from the spectra that the Cu(0.05)-doped $Cd_{0.1}Zn_{0.9}S$ sample prepared by hydrothermal method has higher absorption of Cu^{+} but lower absorption of Cu^{2+} than sample prepared by co-precipitation method. Therefore, it can be proposed that the difference in the absorption spectrum at range of 600–800 nm would be due to difference in the amount of Cu^{2+} species after Cu doping. However, at present, the mechanism for this phenomenon is still unclear.

A plot of $(F(R)h\nu)^2$ *vs* $h\nu$, known as Tauc Plot, was used in order to determine band gap energy of the samples from the absorption spectra, as shown in Figs. 8 and 9. The band gap energy can be determined from the intercept of linear extrapolation with the abscissa axis. The calculated values of the band gap energies for all samples prepared by hydrothermal and co-precipitation methods are listed in Table 1. The values of the band gap energy for $Cd_{0.1}Zn_{0.9}S$ samples determined by the Tauc plot are in good agreement with the value reported in other literature [4]. It was obtained that the band gap energy decreased as the amount of Cu dopant increased. The band gap energy of Cu-doped $Cd_{0.1}Zn_{0.9}S$ samples was smaller than that of the undoped $Cd_{0.1}Zn_{0.9}S$, indicating that Cu-doped samples can utilize a wider spectral region of visible light than the undoped sample.

$Cd_{0.1}Zn_{0.9}S$ sample prepared by hydrothermal method has a lower band gap compared to $Cd_{0.1}Zn_{0.9}S$ sample prepared by co-precipitation method. However, when Cu was doped onto $Cd_{0.1}Zn_{0.9}S$, all of Cu-doped $Cd_{0.1}Zn_{0.9}S$ prepared by hydrothermal

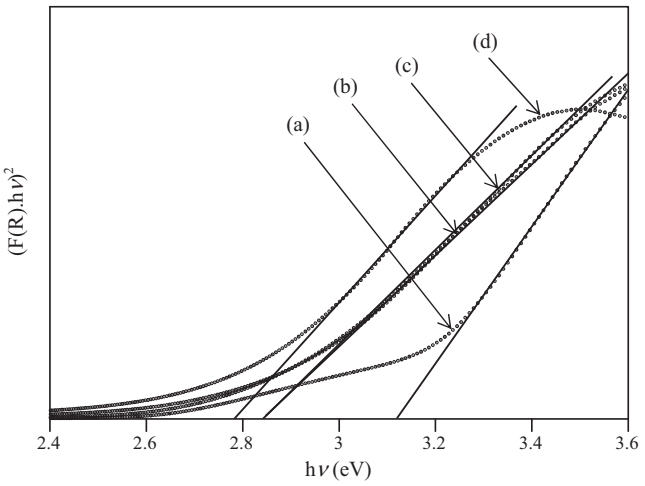

Fig. 8. Tauc Plot of (a) $Cd_{0.1}Zn_{0.9}S$, (b) Cu(0.01)-doped $Cd_{0.1}Zn_{0.9}S$, (c) Cu(0.03)-doped $Cd_{0.1}Zn_{0.9}S$, and (d) Cu(0.05)-doped $Cd_{0.1}Zn_{0.9}S$ prepared by hydrothermal method.

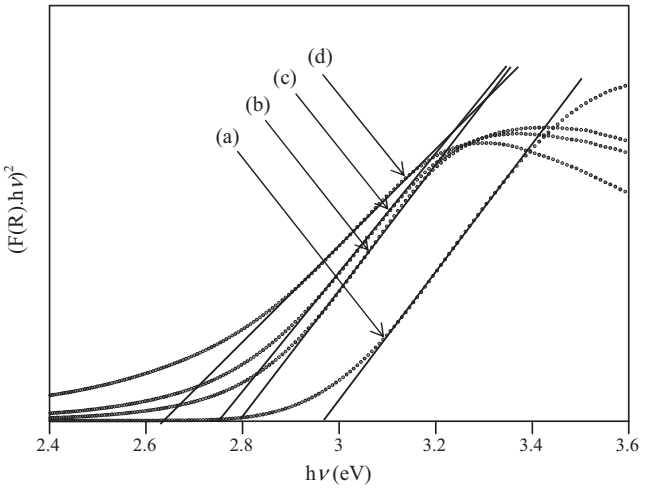

Fig. 9. Tauc Plot of (a) $Cd_{0.1}Zn_{0.9}S$, (b) Cu(0.01)-doped $Cd_{0.1}Zn_{0.9}S$, (c) Cu(0.03)-doped $Cd_{0.1}Zn_{0.9}S$, and (d) Cu(0.05)-doped $Cd_{0.1}Zn_{0.9}S$ prepared by co-precipitation method.

method showed higher band gap energies compared to Cu-doped $Cd_{0.1}Zn_{0.9}S$ prepared by co-precipitation method. The difference in the band gap energy would be originated from the difference in the crystal structure. From this result, it is clear that different preparation method gave different properties on the samples.

3.3. Photocatalytic activity

Even though CdS might be present in the samples prepared by hydrothermal method, the photocatalytic activity will not be greatly influenced. As also shown in the reported paper [11], unmodified CdS almost did not show activity for hydrogen production. Therefore, we can ignore the effect of CdS impurity in the photocatalytic activity.

The photocatalytic activity of the samples prepared by hydrothermal method was examined for hydrogen production as shown in the first run of Fig. 10. The $Cd_{0.1}Zn_{0.9}S$ and Cu-doped $Cd_{0.1}Zn_{0.9}S$ samples are active to produce hydrogen under visible light irradiation. The $Cd_{0.1}Zn_{0.9}S$ sample produced hydrogen with rate of 2.49 mmol/h. It is worthy noted that all Cu-doped $Cd_{0.1}Zn_{0.9}S$ samples showed higher activity than the undoped sample. As the amount of Cu dopant increased, the photocatalytic activity for hydrogen evolution was also increased. The highest hydrogen production rate was 4.37 mmol/h that was obtained on Cu(0.05)-doped $Cd_{0.1}Zn_{0.9}S$ sample. The observed enhanced activity would be due to the higher crystallinity and improved photoabsorption property of the doped samples than the undoped one. Higher crystallinity could lead to fewer defects that act as recombination site, thus, improve the charge separation that resulted in the improvement of photocatalytic activity. On the other hand, the improved photoabsorption was due to the Cu 3d level that formed donor level above the valence band [12,13,28,32,33]. Electrons can be excited from this Cu 3d level to the conduction band, which lowers the band gap energy making it easier for electrons to be excited to the conduction band. This would increase the amount of electrons since more electrons could be generated on the photocatalyst after being irradiated with light and more electrons could participate in the photocatalytic reactions, thus, increase the photocatalytic activity.

In order to check the stability of the samples, the samples were reused as photocatalyst and the photocatalytic activities were shown as second run in Fig. 10. It is clear that the $Cd_{0.1}Zn_{0.9}S$ sample showed much lower activity than that observed in the first run, suggesting the poor stability of the undoped sample. On the other hand, Cu(0.01)-doped $Cd_{0.1}Zn_{0.9}S$ and Cu(0.03)-doped

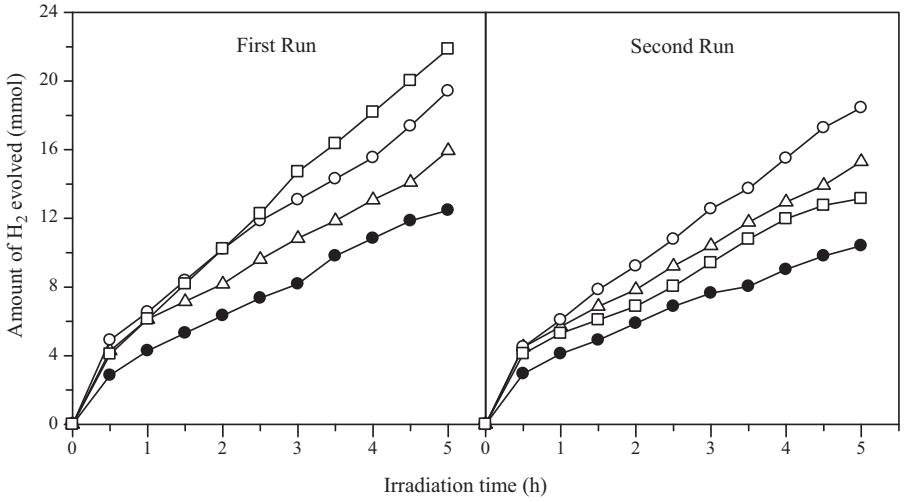

Fig. 10. Photocatalytic hydrogen evolution on $Cd_{0.1}Zn_{0.9}S$ (●), Cu(0.01)-doped $Cd_{0.1}Zn_{0.9}S$ (△), Cu(0.03)-doped $Cd_{0.1}Zn_{0.9}S$ (○), and Cu(0.05)-doped $Cd_{0.1}Zn_{0.9}S$ (□) prepared by hydrothermal method under visible light irradiation.

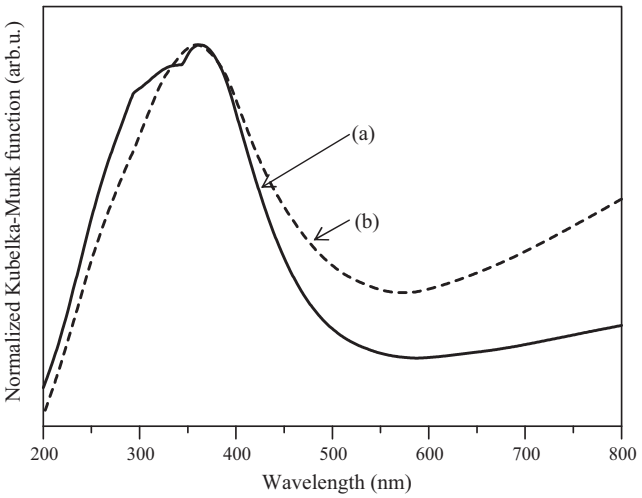

Fig. 11. DR UV–vis spectra of Cu(0.05)-doped $Cd_{0.1}Zn_{0.9}S$ prepared by hydrothermal method (a) before and (b) after reaction.

$Cd_{0.1}Zn_{0.9}S$ still showed high photocatalytic activities that were in the similar level to those obtained in the first run. Unfortunately, Cu(0.05)-doped $Cd_{0.1}Zn_{0.9}S$ showed a significant decrease in the photocatalytic activity. These results suggested that the doping of Cu in a small amount could improve the stability of $Cd_{0.1}Zn_{0.9}S$, while the stability of the sample became poor as the amount of Cu dopant increased.

The poor stability of the Cu(0.05)-doped $Cd_{0.1}Zn_{0.9}S$ sample was also clearly observed from the change of the color from green to grey after the photocatalytic reaction. The DR UV–vis spectra of the sample before and after the second run of reaction are shown in Fig. 11. It was obtained that there were an increase in the absorption more than 600 nm due to the formation of Cu^{2+} species after the reaction and a decrease in the absorption of UV up to 320 nm due to the decrease of Cu^{+}. It can be suggested that the photocorrosion might occur in this sample. Even though the gradual decrease was not clearly observed in the first run, it could be clearly observed in the second run; the activity in the first hour of second run showed similar level to those obtained in the first run, however, gradual decrease started after 1 h-reaction and pronouncedly observed after 3.5 h. From first and second runs, it was confirmed that among the samples, the Cu(0.03)-doped $Cd_{0.1}Zn_{0.9}S$ sample showed the highest photocatalytic activity with hydrogen production rate of 3.86 mmol/h, which was 1.7 times fold of the undoped $Cd_{0.1}Zn_{0.9}S$. The Cu(0.03)-doped $Cd_{0.1}Zn_{0.9}S$ sample also showed high stability for hydrogen production under visible light irradiation.

The photocatalytic activity for hydrogen production on the samples prepared by co-precipitation method was evaluated, as can be seen as first run in Fig. 12. Similar to the results on the samples prepared by hydrothermal method, the addition of Cu into $Cd_{0.1}Zn_{0.9}S$ prepared by co-precipitation method also improved the photocatalytic activity of the sample. The photocatalytic activity of Cu(0.01)-$Cd_{0.1}Zn_{0.9}S$ increased slightly from the undoped $Cd_{0.1}Zn_{0.9}S$. The highest photocatalytic activity was observed on the Cu(0.03)-$Cd_{0.1}Zn_{0.9}S$ with hydrogen production rate of 2.31 mmol/h. The photocatalytic activity decreased slightly when the amount of Cu-doped was 0.05. The lower photocatalytic activity observed here may be due to the lower crystallinity of the samples. The lower crystallinity might lead to more defect sites that act as recombination centres.

For the second run, all of the Cu-doped samples still showed higher photocatalytic activity than $Cd_{0.1}Zn_{0.9}S$. However, the gradual decrease was observed on the Cu(0.01)-$Cd_{0.1}Zn_{0.9}S$ prepared by co-precipitation method as compared to sample prepared by hydrothermal method with the same amount of Cu dopant. The Cu(0.01)-$Cd_{0.1}Zn_{0.9}S$ prepared by co-precipitation method showed almost similar level activity to that of the undoped $Cd_{0.1}Zn_{0.9}S$ in the second run, suggesting that the dopant amount was too low in this case. On the other hand, the photocatalytic activity of Cu(0.03)-$Cd_{0.1}Zn_{0.9}S$ was maintained steady for both runs, while the Cu(0.05)-doped $Cd_{0.1}Zn_{0.9}S$ showed as slightly decrease in the second run. These results suggested that there was an optimum amount for the dopant. It has been reported that both increasing and decreasing of Cu dopant amount gave a great effect on the photocatalytic performance [11]. From the comparison of activity and stability of samples prepared by hydrothermal and co-precipitation methods it can be proposed here that regardless the preparation methods, the sample with optimum amount of dopant will give both high photocatalytic activity and stability.

Comparison to the previously reported $Cd_{0.1}Sn_xZn_{0.9-2x}S$ solid solutions [17], the present Cu-doped $Cd_{0.1}Zn_{0.9}S$ solid solutions showed slightly higher photocatalytic activity of *ca.* 10% under the same reaction condition at optimum amount of dopant. It might be due to the fact that the Cu-doped $Cd_{0.1}Zn_{0.9}S$ solid solutions have better absorption in the visible light region than the $Cd_{0.1}Sn_xZn_{0.9-2x}S$ solid solution. This study again clearly shows that

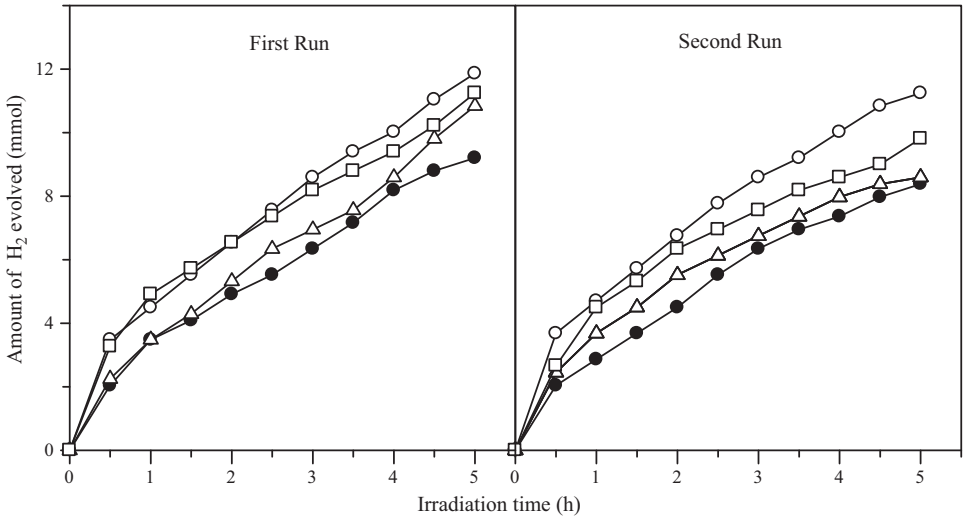

Fig. 12. Photocatalytic hydrogen evolution on $Cd_{0.1}Zn_{0.9}S$ (●), Cu(0.01)-doped $Cd_{0.1}Zn_{0.9}S$ (△), Cu(0.03)-doped $Cd_{0.1}Zn_{0.9}S$ (○), and Cu(0.05)-doped $Cd_{0.1}Zn_{0.9}S$ (□) prepared by co-precipitation method under visible light irradiation.

the addition of third metal ion is an effective way to improve the photocatalytic activity and stability of the $Cd_{0.1}Zn_{0.9}S$ solid solutions. The possibility to use other metal ions is currently under investigation.

4. Conclusions

Highly active and stable Cu-doped $Cd_{0.1}Zn_{0.9}S$ sample for hydrogen production under visible light irradiation can be prepared by hydrothermal method. It was obvious that preparation methods significantly influenced the properties and photocatalytic performance of photocatalyst. Compared to co-precipitation method, hydrothermal method is a better way to prepare efficient and stable Cu-doped $Cd_{0.1}Zn_{0.9}S$ photocatalysts under mild temperature. The highest photocatalytic activity with high stability was observed on the Cu(0.03)-doped $Cd_{0.1}Zn_{0.9}S$ sample with hydrogen rate of 3.86 mmol/h, which was 1.7 times higher than the undoped sample. It was suggested that the high activity and stability was due to optimum amount of Cu dopant, the high crystallinity, as well as the narrow band gap energy.

Acknowledgement

Financial support from the Ministry of Science, Technology and Innovation through the National Science Fellowship is greatly acknowledged (MK).

References

[1] J.F. Reber, M. Rusek, J. Phys. Chem. 90 (1986) 824–834.
[2] H.C. Youn, S. Baral, J. Fendler, J. Phys. Chem. 92 (1988) 6320–6327.
[3] G. De, A. Roy, S. Bhattacharya, Int. J. Hydrogen Energy 21 (1996) 19–23.
[4] C. Xing, Y. Zhang, W. Yan, L. Guo, Int. J. Hydrogen Energy 31 (2006) 2018–2024.
[5] A. Roy, G. De, J. Photochem. Photobiol. A 157 (2003) 87–92.
[6] A. Kudo, M. Sekizawa, Catal. Lett. 58 (1999) 241–243.
[7] A. Kudo, M. Sekizawa, Chem. Commun. (2000) 1371–1372.
[8] I. Tsuji, A. Kudo, J. Photochem. Photobiol. A 156 (2003) 249–252.
[9] I. Tsuji, H. Kato, H. Kobayashi, A. Kudo, J. Am. Chem. Soc. 126 (2004) 13406–13413.
[10] W. Zhang, R. Xu, Int. J. Hydrogen Energy 34 (2009) 8495–8503.
[11] W. Zhang, Z. Zhong, Y. Wang, R. Xu, J. Phys. Chem. C 112 (2008) 17635–17642.
[12] G. Liu, L. Zhao, L. Ma, L. Guo, Catal. Commun. 9 (2008) 126–130.
[13] G. Liu, Z. Zhou, L. Guo, Chem. Phys. Lett. 509 (2011) 43–47.
[14] X. Zhang, D. Jing, M. Liu, L. Guo, Catal. Commun. 9 (2008) 1720–1724.
[15] X. Zhang, D. Jing, L. Guo, Int. J. Hydrogen Energy 35 (2010) 7051–7057.
[16] J.A. Villoria, R.M.N. Yerga, S.M. Al-Zahrani, J.L.G. Fierro, Ind. Eng. Chem. Res. 49 (2010) 6854–6861.
[17] M. Kimi, L. Yuliati, M. Shamsuddin, Int. J. Hydrogen Energy 36 (2011) 9453–9461.
[18] K. Zhang, D. Jing, C. Xing, L. Guo, Int. J. Hydrogen Energy 32 (2007) 4685–4691.
[19] S. Zu, Z. Wang, B. Liu, X. Fan, G. Qian, J. Alloys Compd. 476 (2009) 689–692.
[20] S. Sain, S.K. Pradhan, J. Alloys Compd. 509 (2011) 4176–4184.
[21] G. Zhang, X. Zou, J. Gong, F. He, H. Zhang, S. Ouyang, H. Liu, Q. Zhang, Y. Liu, X. Yang, B. Hu, J. Mol. Catal. A: Chem. 255 (2006) 109–116.
[22] J.L. Ferrari, M.A. Cebim, A.M. Pires, M.A. Couto dos Santos, M.R. Davolos, J. Solid State Chem. 183 (2010) 2110–2115.
[23] R. Mariappana, M. Ragavendarb, V. Ponnuswamya, J. Alloys Compd. 509 (2011) 7337–7343.
[24] W. Wong, W. Zhu, H. Xu, J. Phys. Chem. C 112 (2008) 16754–16758.
[25] X. Qiu, M. Miyauchi, H. Yu, H. Irie, K. Hashimoto, J. Am. Chem. Soc. 132 (2010) 15259–15267.
[26] A. Datta, S.K. Panda, S. Chaudhuri, J. Solid State Chem. 181 (2008) 2332–2337.
[27] L.S. Yoong, F.K. Chong, B.K. Dutta, Energy 34 (2009) 1652–1661.
[28] J. Sun, G. Chen, Y. Li, C. Zhao, H. Zhang, J. Alloys Compd. 509 (2011) 1133–1137.
[29] R. Chand, E. Obuchi, K. Katoh, H.N. Luitel, K. Nakano, Catal. Commun. 13 (2011) 49–53.
[30] G. Colon, M. Maicu, M.C. Hidalgo, J.A. Navio, App. Catal. B Environ. 67 (2006) 41–51.
[31] H. Praliaud, S. Mikhailenko, Z. Chajar, M. Primet, Appl. Catal. B 16 (1998) 359–374.
[32] H. Zhang, G. Chen, X. Li, Q. Wang, Int. J. Hydrogen Energy 34 (2009) 3631–3638.
[33] K.G. Kanade, B.B. Kale, J. Baeg, S.M. Lee, C.W. Lee, S. Moon, H. Chang, Mater. Chem. Phys. 102 (2007) 98–104.